

Fast Neutron Emission from a High-Energy Ion Beam Produced by a High-Intensity Subpicosecond Laser Pulse

L. Disdier,¹ J-P. Garçonnet,¹ G. Malka,² and J-L. Miquel²

¹*Commissariat à l'Energie Atomique, Bruyères le Châtel, BP 12, 91680 Bruyères le Châtel, France*

²*Commissariat à l'Energie Atomique, Limeil-Valenton, 94195 Villeneuve-Saint-Georges Cedex, France*

(Received 5 March 1998)

Neutron emission as high as 10^7 is observed when a high intensity (a few 10^{19} W/cm²) subpicosecond laser pulse at 529 nm wavelength is focused on a deuterated polyethylene target. Neutron emission is also measured in different directions. The emission of neutrons along the laser axis is higher than in the transverse direction. Nonisotropic emission is consistent with neutrons generated by $D(d, n)^{-3}\text{He}$ reaction for 0.3–1 MeV deuterons accelerated in the direction of the laser beam. The energy transferred to the ions is roughly estimated and compared with the energy carried out by the electrons. [S0031-9007(98)08299-4]

PACS numbers: 52.40.Nk, 52.50.Jm, 52.70.Nc

The development of chirped pulse amplification has made possible the generation of energetic subpicosecond laser pulses [1]. The interaction of the laser pulse with a target generates energetic particles, like MeV electrons and ions [2]. The fast ignitor concept [3], relevant to the inertial confinement fusion (ICF), enhances the interest in this process: Hot particles could heat to thermonuclear temperature an already compressed deuterium-tritium fuel.

High-intensity subpicosecond laser pulses produce fast neutrons when they interact with a deuterated target [4]. Hot deuterium ions create neutrons from $D(d, n)^{-3}\text{He}$ reaction. Measurements of this neutron emission is a useful method to diagnose fast ions (in the keV to MeV range) generated by the interaction of the laser with the target. Particle-in-cell (PIC) calculations show that high-energy ions are accelerated by a shock wave propagating inside the target [5–7]. It knocks the ions along the direction of the laser propagation [8], but collisions stop the ions in the thickness of the target. Neutron emission can identify these ions which cannot be directly measured.

Here, we report neutron emission from a deuterated polyethylene target irradiated with a subpicosecond 529 nm laser. The focused intensity is a few 10^{19} W/cm². The experimental conditions are similar to other experiments [1,9]. The laser system provides a chirped pulse with energies up to 30 J at the fundamental wavelength of 1.058 μm . After compression by a pair of diffraction gratings, the pulse duration, measured by an autocorrelation method, is routinely 400 fs. A KH_2PO_4 (KDP) crystal is used to convert the laser beam to 529 nm with an efficiency of 70%. The pulse duration is less than 300 fs. An $f/3$ off-axis parabolic mirror focuses the laser pulse to a 5- μm -diameter spot containing about 30% of the total energy. The highest intensity is 3.5×10^{19} W/cm² for a laser energy of 7 J at 529 nm.

At 1.058 μm , the contrast ratio measured at a few tens of picosecond before the main pulse by a third order cross correlator is 10^8 . Three dichroic mirrors located after the

KDP crystal increase the contrast ratio to 10^{12} at 529 nm. The optical intensity before the pulse is insufficient to ionize the target, so the pulse interacts directly with the solid target and not with a plasma.

The target is made from deuterated polyethylene powder compressed to solid density. The compressed disk has a density of $1 \text{ g/cm}^3 \pm 10\%$ and is $400 \pm 50 \mu\text{m}$ thick. The composition of the $(\text{CD}_2)_n$ target, analyzed by nuclear magnetic resonance, is 92% of deuterium and 8% of hydrogen by atom.

Neutrons are detected by the $^{10}\text{B}(n, \alpha)^7\text{Li}$ reaction in a BF_3 detector. The BF_3 tube (5 cm in diameter, 45 cm in active length) is located inside a cylinder made of polyethylene (0.7 m in length, 15 cm in diameter, 5 cm in thickness). The counter is shielded with a 5 mm thick lead sheet. Fast neutrons are slowed to thermal energy in the polyethylene moderator before interacting with the boron. Neutrons are discriminated against MeV photons by pulse height. The detector sensitivity is nearly independent of neutron energy in the 0.1 to 6 MeV range [10]. For neutrons in the eV range, the sensitivity is limited by transmission of the polyethylene and the lead sheet (4×10^{-3}).

The BF_3 detectors are calibrated with an AmBe neutron source emitting 1.42×10^5 neutrons/sec. This source is located at the center of the interaction chamber, and the counting time is 300 sec. We perform the same measurements without the neutron source in place to estimate the contribution of the background. The contribution of the background to the neutron count is at maximum 20% and is subtracted from the total counts measured with a neutron source. The sensitivity of the counters is expressed in terms of the number of source neutrons per count detected. The same calibration procedure is done with a Cf^{252} fission source with an energy spectrum centered at 2 MeV. This energy is close to the neutron energy of the $D(d, n)^{-3}\text{He}$ reaction. The calibration coefficients from the two procedures agree to within 10%.

Experimentally, we count for a period of 500 μs after the laser pulse. Signals in the first μs which are compromised by electromagnetic noise and direct x-ray emission interaction into the tube are not included in the data. Most of the counts occur in the first 250 μs which corresponds to the response time of the detector; no neutrons are detected after 500 μs . Correction due to background is negligible because the counting time is short. The experimental error is mainly due to statistical fluctuations: The accuracy of the measurements depends on the number of counts detected and is typically 10%–50% (standard deviation).

Figure 1 shows the positions of BF_3 detectors for measuring the polar diagram of the emission. Detectors at 0° , 20° , 45° , 67.5° , and 100° detectors are located at 5, 5.4, 1.6, 2.5, and 2.1 m, respectively, from the center of the experimental chamber. In the experiments, the laser beam is at normal incidence on the target. Neutron emission is detected only when the irradiated target contains deuterium; no neutrons are detected from aluminum or gold targets. This test verifies that the signal observed in the range of the detectors is not produced by high-energy photons or induced by the photoneutron process on the wall of the chamber. Production of neutrons with energies below 1 eV is also excluded. Indeed, the time delay for those neutrons to reach a detector at 5 m is greater than 360 μs , whereas most of the counts are detected within 250 μs after the laser shot.

For most of the shots, the highest emission level is measured by the detector at 0° relative to the laser axis. This emission appears to be very dependent on laser illumination conditions, as shown in Fig. 2. For an intensity of $3.5 \times 10^{19} \text{ W/cm}^2$, the neutron emission level in the direction along the laser axis reaches the value of $7.5 \times 10^6/4\pi$ compared to $5 \times 10^5/4\pi$ for a laser intensity of $2 \times 10^{19} \text{ W/cm}^2$. For the same laser energy at 1.058 μm , this strong intensity dependence results in large shot to shot variations in the neutron

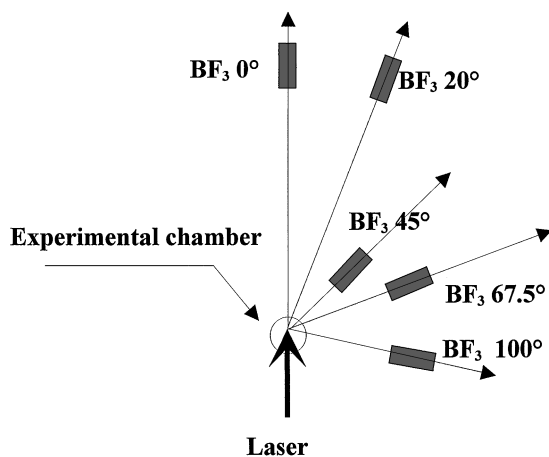


FIG. 1. Top view of the experimental setup.

production, attributable to small variations in the flux at 529 nm. The highest level of neutron emission ($10^7/4\pi$) requires the maximum laser intensity at 529 nm which is difficult to reproduce because of fluctuations in the wavelength conversion efficiency. We concentrate on the characterization of the interaction for the typical laser flux of $2 \times 10^{19} \text{ W/cm}^2$, for which the neutron yield is from 10^5 to 10^6 . These levels of neutrons and laser flux are routinely obtained on the facility.

Fast electron levels and spectra are also measured using a magnetic spectrometer located 16.5 cm behind the target in the direction of the laser axis. This diagnostic [1] measures the number of electrons at six different energies, namely, 492, 899, 1326, 1762, 2203, and 2647 keV. The electrons traverse the 400 μm thick target before detection; the loss in the target is estimated to be 72 keV from the Bethe formula for the fast electrons. Typical spectra of electrons—not corrected for these losses—are presented in Fig. 3 for several laser intensities. The shape of the spectrum is non-Maxwellian for laser intensities above $0.6 \times 10^{19} \text{ W/cm}^2$.

The level of neutron emission is strongly correlated with the energy transferred to the electrons. This energy is obtained by integrating the spectrum of electrons between 492 and 2647 keV; it is typically a few mJ/sr, which is close to previous measurements [1]. In Fig. 4, for example, the neutron flux measured with the 45° counter is plotted versus the energy in the fast electrons. A least-squares approximation shows that the dependence of the neutron flux, $N_n(45^\circ)$, on the energy in the electrons E_e (in mJ/sr) is nearly exponential: $N_n(45^\circ) = 2 \times 10^4 \times \exp(1.2 \times E_e)$. Measurements at other angles show a similar variation.

There is a clear correlation between the neutron emission and the generation of energetic electrons. The energy carried away by the fast electrons provides a measure of the strength of the laser-target interaction that takes into

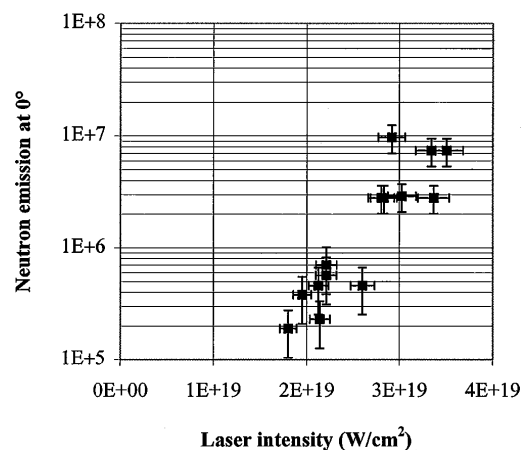


FIG. 2. Measured neutron emission (extrapolated into 4π) in the direction along the laser axis versus the laser intensity.

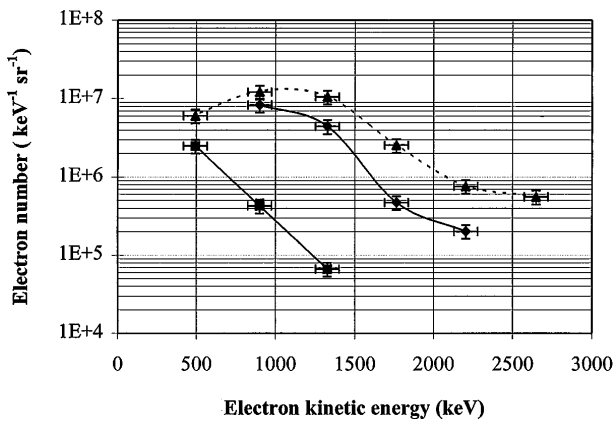


FIG. 3. Electron distribution from 500 to 3000 keV for laser intensities $0.6 \times 10^{19} \text{ W/cm}^2$ (squares), $1.3 \times 10^{19} \text{ W/cm}^2$ (diamonds), and $2.7 \times 10^{19} \text{ W/cm}^2$ (triangles), measured along the laser propagation axis in the forward direction.

account local variations in the laser flux during the interaction: for instance, laser filamentation.

To improve the accuracy of our analysis, we average the neutron measurement obtained with each detector over all the shots with the same measured energy in the electrons; for example, eight laser shots are available for an energy of $2 \text{ mJ/sr} \pm 10\%$. This procedure decreases the fractional standard deviation to $\pm 20\%$ at maximum. The resulting semipolar diagram of neutron emission is shown in Fig. 5. The neutron flux at 0° is 3 times larger than the flux at 90° . The mean laser intensity for these shots is $2.3 \times 10^{19} \text{ W/cm}^2$.

Recent simulations show that high-energy ions are accelerated preferentially in the direction of the laser beam [7] and suggest a beam-target type of interaction. A deuteron beam impacting a solid thick CD_2 target generates an anisotropy in the neutron emission that depends

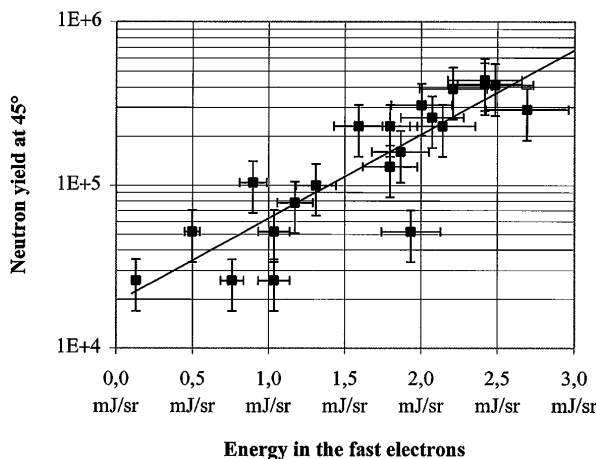


FIG. 4. Measured neutron emission (extrapolated into 4π) in the direction at 45° to the laser axis versus the energy carried away by the 0.5–3000 keV electrons.

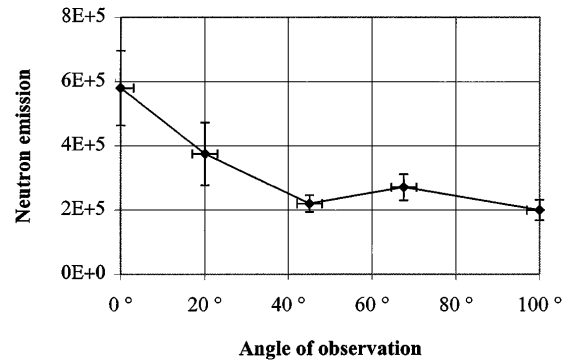


FIG. 5. Neutron emission (extrapolated into 4π) versus the angle of the BF_3 detectors. The data points represent an average of eight measurements, each of which had the same total energy $2.2 \text{ mJ/sr} \pm 10\%$ in the 0.5–3000 keV electrons.

on the energy of the ions [11]. For a detector located at an angle θ relative to the direction of a deuteron beam of energy E_d , the neutron emission $Y(\theta, E_d)$ collected per incident deuteron is given by

$$Y(\theta, E_d) = \int_0^{E_d} \frac{\sigma(\theta, E)}{\varepsilon(E)} dE, \quad (1)$$

where σ is the differential cross section for the $\text{D}(d, n)^3\text{He}$ reaction, and ε is the stopping cross section for deuterons per atom of deuterium. The neutron emission depends on the angle of observation through the variation of the differential cross section with θ . In Fig. 6, the neutron flux calculated with Eq. (1) versus θ and normalized with the emission at 0° is presented for different deuteron beam energies (E_d). The values for σ and ε from [11,12] are used. We also plot the experimental neutron emission versus the angle of observation. We conclude that the observed neutrons are produced by ions with a mean energy of 550 keV. In Fig. 7, we present

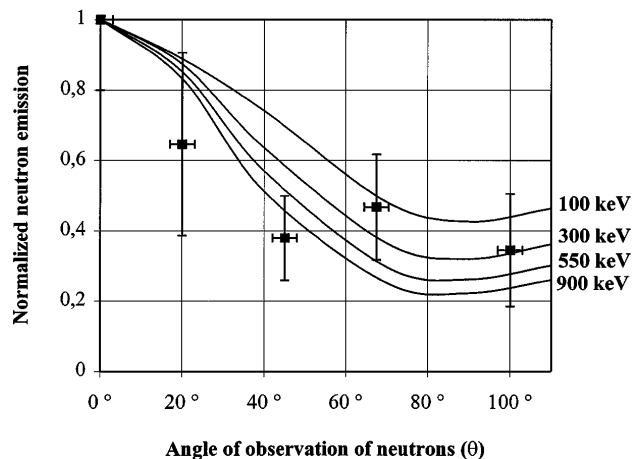


FIG. 6. Normalized neutron emission versus angle of observation as estimated from (1) for 100, 300, 550, and 900 keV monoenergetic deuterons. Squares: experimental data.

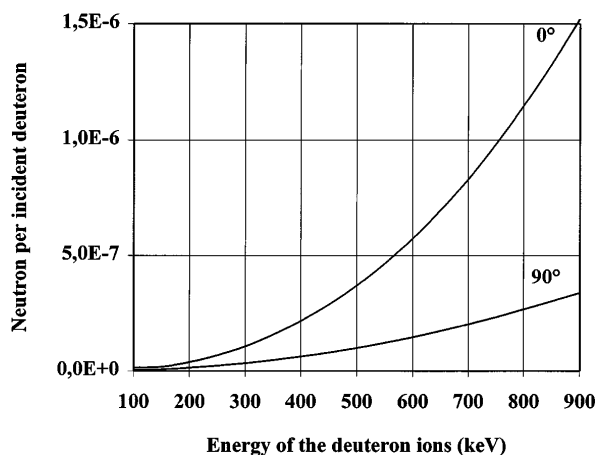


FIG. 7. Neutron emission per incident ion versus the energy of the deuterons at 0° and 90° from the direction of the ion beam, estimated from (1).

the neutron yield per incident deuteron at 0° and at 90° versus the ion energy. From these graphs, we deduce that 10^{11} deuterons at 550 keV are necessary to create the $6 \times 10^5/4\pi$ neutrons measured in the direction of the laser axis. The energy transferred to these ions is 9 mJ, nearly the same as the energy in the fast electrons.

The accuracy of this analysis is difficult to establish. A precise determination of the energy of the ions requires an increase in the accuracy of the neutron measurement and inclusion of the angular spread of the ion beam. The 2D PIC calculations including these effects are in progress [13]. However, only ions from 0.3 to 1 MeV of energy could clearly account from the neutron anisotropy that we observed. The variation of the neutron emission with θ demonstrates that high-energy ions are accelerated in the direction of the laser. The analysis shows also that significant energy is transferred to those ions, compared to the energy coupled to the fast electrons.

Neutron emission could originate from other physical mechanisms. Bremsstrahlung photons with energy up to 2.2 MeV also produce photoneutrons by (γ, n) reaction with deuterium. However, the efficiency is low: 1 photon in 10^6 to 10^7 interacts to produce 1 neutron [10]. For these experiments, the number of electrons with energies up to 2.2 MeV is about 6×10^8 per steradian. That leads to a rough estimate of 10^1 to 10^2 neutrons created by such a process. This is negligible compared to the yield measured.

Moreover, some recent measurements obtained with a first hit neutron spectrometer show that the neutron time of flight is consistent with 2.5 MeV neutrons. This spectrometer [14] is made on the LaNSA model [15]. It is composed of an array of 96 fluor detectors similar to those used for MEDUSA [16]. The detectors are calibrated against a test exposure of a known 2.5 MeV neutron flux. Hard x rays produced by the interaction saturate the plastic scintillators of the detectors. Therefore, the spectrom-

eter must be placed 2.5 m away from the experimental chamber. In this condition, only a few scintillators detect an event for a neutron yield of 5×10^5 . The number of events recorded is in agreement with the yield measured by the BF_3 detectors. These events show that the times of flight correspond to a neutron of 2.5 MeV but they are not sufficient to provide a spectrum.

In conclusion, we have measured the neutron emission created by a high-intensity laser pulse with a high contrast ratio focused on a deuterated target. The neutron yield is strongly dependent on the laser intensity and can reach $10^7/4\pi$ along the laser axis at high laser intensity ($>3 \times 10^{19}$ W/cm²). It is also strongly correlated with the energy carried away by the fast electrons. The neutron energies measured by a single hit spectrometer confirm that the neutrons originate from the $\text{D}(d, n)^3\text{He}$ nuclear reaction. The anisotropic distribution of the neutrons suggests ions of at least 550 keV based on a beam target model interaction. We plan to use D^7Li targets in which high-energy ion beams produce 10.8 and 13.3 MeV neutrons via the $^7\text{Li}(d, n)^8\text{Be}$ nuclear reaction (the reaction threshold is for 400 keV ions) to confirm this result.

We thank G. Bonnaud, E. Lefebvre, C. Toupin, and M. Louis-Jacquet for fruitful discussions. We also acknowledge the technical assistance of the P102-Castor staff at CEA Limeil.

-
- [1] N. Blanchot *et al.*, Opt. Lett. **20**, 395 (1995); C. Rouyer *et al.*, J. Opt. Soc. Am. B **13**, 55 (1996).
 - [2] G. Malka and J.L. Miquel, Phys. Rev. Lett. **77**, 75 (1996).
 - [3] M. Tabak *et al.*, Phys. Plasmas **1**, 1626 (1994).
 - [4] P.A. Norreys *et al.*, Plasma Phys. Controlled Fusion **40**, 175 (1998).
 - [5] J. Denavit, Phys. Rev. Lett. **69**, 3052 (1992).
 - [6] S.C. Wilks *et al.*, Phys. Rev. Lett. **69**, 1383 (1992).
 - [7] S. Miyamoto *et al.*, J. Plasma Fusion Res. **73**, 343 (1997).
 - [8] E. Lefebvre, Ph.D. thesis, Paris Sud University, 1996 (unpublished).
 - [9] T. Feurer *et al.*, Phys. Rev. E **56**, 4608 (1997).
 - [10] G.F. Knoll, *Radiation Detection and Measurement* (J. Wiley & Sons, New York, 1979).
 - [11] J.B. Marion and J.L. Fowler, *Fast Neutron Physics* (Interscience Publishers Ltd., London, 1960).
 - [12] F.C. Young *et al.*, N.R.L. Memo Report No. 3823; H. Liskien and A. Paulsen, At. Data Nucl. Data Tables **11**, 569 (1973).
 - [13] C. Toupin *et al.*, in *Proceedings of the International Congress on Plasma combined with the 25th EPS Conference on Controlled Fusion and Plasma Physics, Prague, 1998* (European Physical Society, Prague, 1998), Vol. 22C, p. 914.
 - [14] J.P. Garçonnet *et al.*, Commissariat à l'Énergie Atomique, France (to be published).
 - [15] M.D. Cable *et al.*, Rev. Sci. Instrum. **63**, 4823 (1992).
 - [16] R.E. Chrien *et al.*, Los Angeles National Laboratory Report No. LA-UR-92-0875.